



# Analytical solution of thermoelastic attenuation in fine layering for random variations of the Grüneisen ratio

Zhi-Wei Wang<sup>a,c</sup>, Li-Yun Fu<sup>a,b</sup>, José M. Carcione<sup>d</sup>, Wanting Hou<sup>c</sup>, and Jia Wei<sup>e</sup>

<sup>a</sup>Shandong Provincial Key Laboratory of Deep Oil and Gas, China University of Petroleum (East China), Qingdao, China; <sup>b</sup>Laboratory for Marine Mineral Resources, Qingdao National Laboratory for Marine Science and Technology, Qingdao, China; <sup>c</sup>School of Geosciences, China University of Petroleum (East China), Qingdao, China; <sup>d</sup>National Institute of Oceanography and Applied Geophysics OGS, Trieste, Italy; <sup>e</sup>Key Laboratory of Petroleum Resource Research, Institute of Geology and Geophysics, Chinese Academy of Sciences, Beijing, P. R. China

## ABSTRACT

Thermoelastic attenuation of P waves is due to energy conversion to the heat mode, which is diffusive at low frequencies and wave-like at high frequencies, behaving similarly to the Biot slow mode. The conversion is strong in highly heterogeneous media. We consider a layered medium with a random distribution of thermal properties, specifically the Grüneisen ratio, and obtain the phase velocity and quality factor. The relaxation peak of the random medium is wider than those of a periodic sequence of layers and the Zener mechanical model. Indeed, a Cole–Cole fractional model is needed to obtain a good match. These approximations are required to compute wave fields in heterogeneous media. Moreover, the solutions are helpful for studying the physics of thermoelasticity and testing numerical algorithms for wave propagation.

## ARTICLE HISTORY

Received 9 August 2021  
Accepted 4 December 2021

## KEYWORDS

Thermoelastic dissipation;  
random layered media;  
quality factor; phase velocity

## 1. Introduction

Thermoelasticity extends the classical elasticity theory by coupling the elastic-displacement and temperature fields, describing the conversion from mechanical energy (e.g., waves) to heat and vice versa. This conversion implies a high level of wave attenuation and velocity dispersion in heterogeneous media, a phenomenon that is of interest in geophysics [1–4].

Ref. [5] established the classical theory of thermoelasticity based on the Fourier law of heat conduction, but the theory predicts infinite wave velocities because it is based on a parabolic-type heat equation. Many researchers have developed models to avoid this anomalous behavior by introducing a relaxation term, specifically, the thermoelasticity model proposed by Lord and Shulman in 1967 (L–S) [6], Green and Lindsay in 1972 (G–L) [7], Green and Naghdi in 1993 (G–N) [8], Hetnarski and Ignaczak in 1996 (H–I) [9], Chandrasekharaiah (1998) and Tzou (1995) (C–T) [10, 11]. Recently, Ref. [12] obtained the wave velocities and simulated wavefields based on the L–S model, and Ref. [13] generalized the model to the poroelastic case. Ref. [14] and Ref. [15] derived the Green function of the L–S thermoelasticity and thermo-poroelasticity theories, respectively, and Ref. [16] established a thermo-poroelasticity theory based on the L–S and G–L theories. The single-medium theory predicts three kinds of waves, namely, a fast P wave (E), a slow thermal P wave (T) and a shear wave (S), while the poroelasticity theory has, in

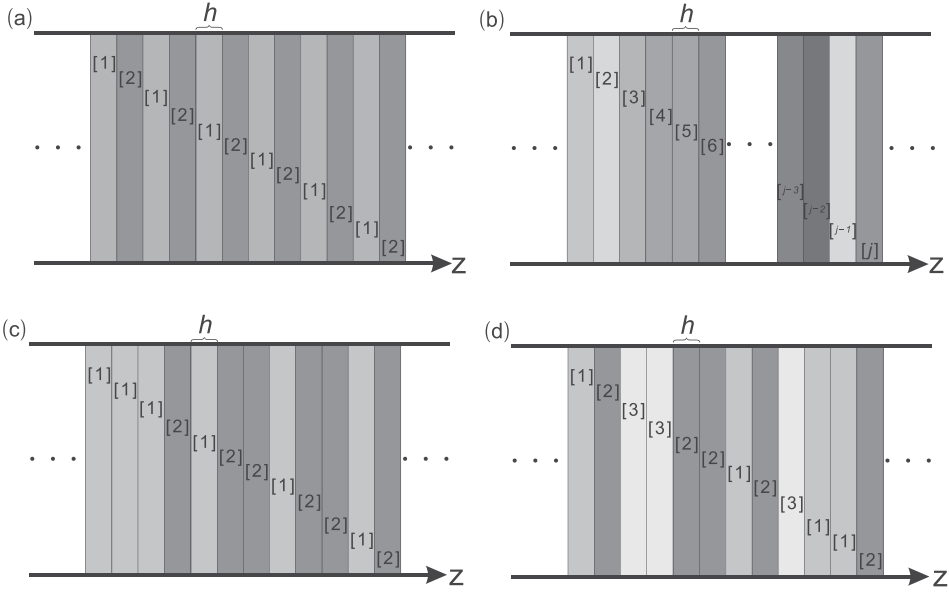


**Figure 1.** Periodic medium with two flat slabs of dissimilar property (a), general random  $h$  medium (b), and random media with two (c) and three (d) slabs of dissimilar property. All the layers have the same thickness  $h$ .

addition, the slow P (Biot) mode. The T wave has characteristics similar to those of the slow Biot mode [12, 14], i.e., diffusive at low frequencies and wave-like at high frequencies.

Formally, the equations of thermoelasticity and poroelasticity have similar structures, since temperature is mathematically equivalent to fluid pressure [17, 18], Ref. [19] extended this formal analogy to attenuation and dispersion [20]. Because the seismic wavelength is much larger than the grain size, a local isostress condition holds, but the presence of different minerals, cracks and cavities induce uneven deformations or strains. This gives rise to temperature variations and related local gradients [21]. Ref. [3] discussed the solution of thermoelastic attenuation of an elastic wave by cracks, while Ref. [4] considered finely layered media. Recently, Ref. [20] analyzed the cases of spherical and cylindrical pores and thin periodic layers, and obtained the respective relaxation peaks of wave attenuation, as well as the velocity dispersion from the Kramers–Kronig relations. However, sedimentary strata present a random distribution of properties. Therefore, we consider the more realistic case of layers with a random distribution of the Grüneisen ratio, i.e., the thermal coefficient to the specific heat ratio. Moreover, the implementation of the physics of wave propagation into numerical modeling in the space-time domain requires approximations by using Zener and Cole–Cole models [22, 23].

The paper is organized as follows. First, we establish the analogy between the diffusion equations of poroelasticity and thermoelasticity, and set the solution proposed by Ref. [4] for a random system. Then, we obtain the attenuation and phase velocity based on the Kramers–Kronig relations [24, 25]. Finally, we approximate the relaxation peak with those of the Zener and Cole–Cole models, and present examples.

## 2. Thermoelasticity theory

### 2.1. Equations of motion

The stress-strain relation in isotropic media is

$$\sigma_{ij} = 2\mu\epsilon_{ij} + (\lambda u_{k,k} - \beta T)\delta_{ij} + f_{ij}, \quad (1)$$

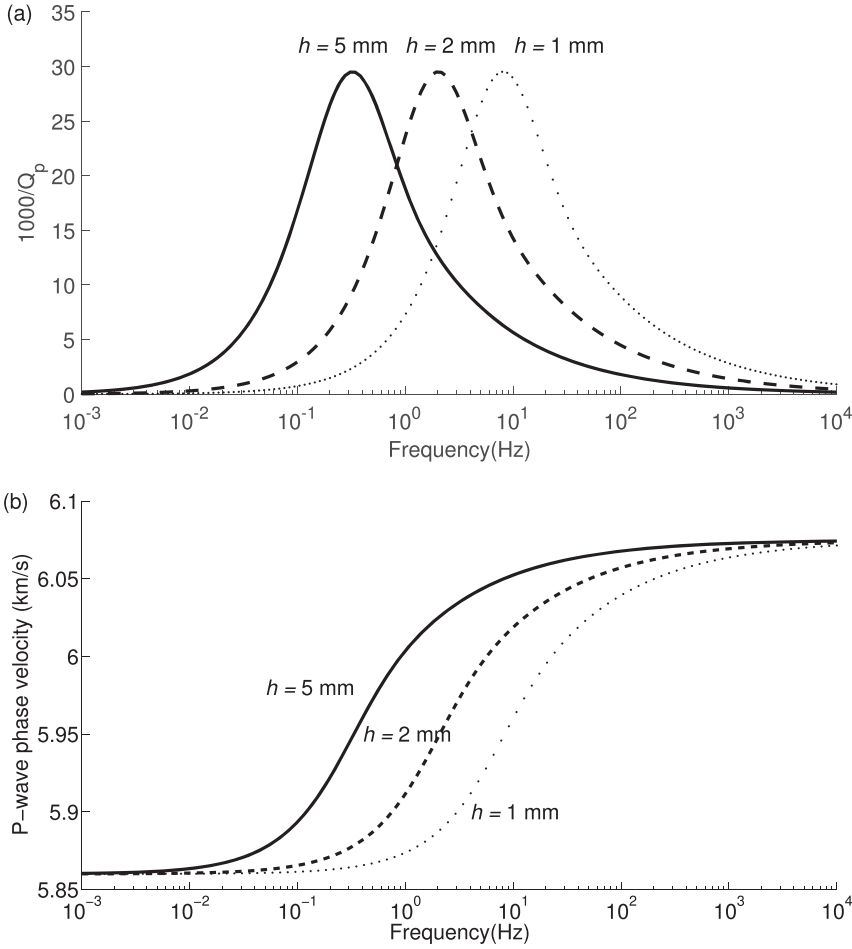


**Figure 2.** Dissipation factor (a) and phase velocity (b) of P waves as a function of frequency for the periodic case and several layer thicknesses.

where  $\sigma_{ij}$  are the stress components,  $T$  is the increment of temperature above a reference absolute temperature  $T_0$ ,  $\lambda$  and  $\mu$  are the Lamé constants,  $\beta = (3\lambda + 2\mu)\alpha$ , where  $\alpha$  is the coefficient of thermal expansion,  $f_{ij}$  are external stress forces,  $\delta_{ij}$  are Kronecker-delta components, and

$$2\epsilon_{ij} = u_{i,j} + u_{j,i}, \quad (2)$$

where  $u_i$  and  $\epsilon_{ij}$  are the components of displacement and strain, respectively.

On the other hand, the equations of momentum conservation are

$$\sigma_{ji,j} = \rho \ddot{u}_i + f_i, \quad (3)$$

where  $f_i$  are external body-force components,  $\rho$  is the mass density, and a dot above a variable denotes time differentiation.

Equations (1) and (3) are complemented by that of heat conduction:

$$\gamma \Delta T = c \dot{T} + \beta T_0 \dot{\epsilon}, \quad (4)$$

where  $\gamma$  is the coefficient of thermal conductivity,  $c$  is the specific heat of the unit volume in the absence of deformation,  $\Delta$  is the Laplacian operator, and  $\epsilon$  is the strain tensor.

There is a mathematical analogy between thermoelasticity and poroelasticity that holds for temperature and fluid pressure, since both fields obey a diffusion equation. Local gradients of

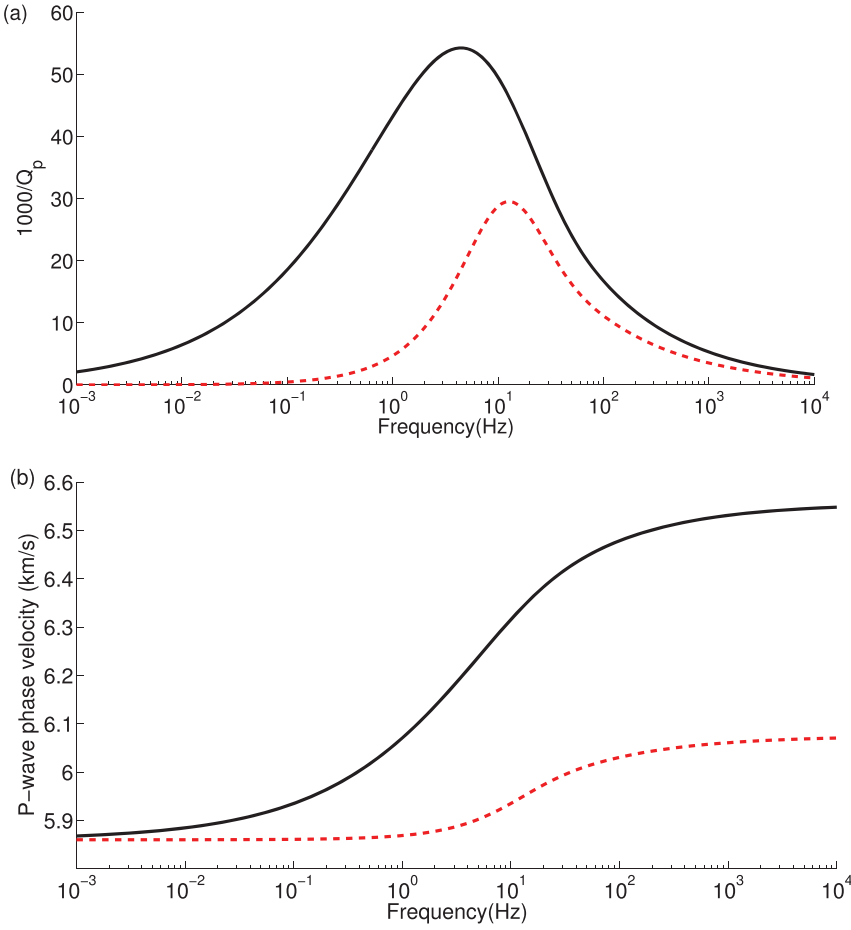


**Figure 3.** Dissipation factor (a) and phase velocity (b) of P-waves as a function of frequency for the random (black-solid) and periodic (red-dashed) cases consisting of two media. The thickness is  $h = 0.8$  mm.

these fields induce attenuation and dispersion of elastic waves [19, 20]. Basically, the slow Biot mode is equivalent to the T wave. In thermoelasticity, we obtain a thermal diffusivity  $d_t = \gamma / (c + \beta^2 T_0 / E)$ , where  $E = \lambda + 2\mu$ , and heat currents induced by stress waves have a diffusion length  $L = \sqrt{d_t / \omega}$ , where  $\omega = 2\pi f$  is the angular frequency,  $f$  is frequency. When this length has the size of the cavities or layers, wave attenuation is maximum, dictating the location of relaxation peaks in the frequency domain.

## 2.2. Quality factor

Thermoelastic damping in polycrystals was explored by Ref. [21]. In this context, Ref. [26] described bulk dissipation within the inner core of the Earth [27]. Since the structure of sedimentary strata is generally approximated by a layered medium [28], Ref. [20] presented a canonical analytical solution of thermoelastic attenuation for periodic layering. A more realistic case is to consider random variations of the thermal properties [4]. The solution is given in Appendix A for a random distribution of the Grüneisen ratio, Appendix B and C illustrate approximations based on the Zener and Cole–Cole models, respectively.

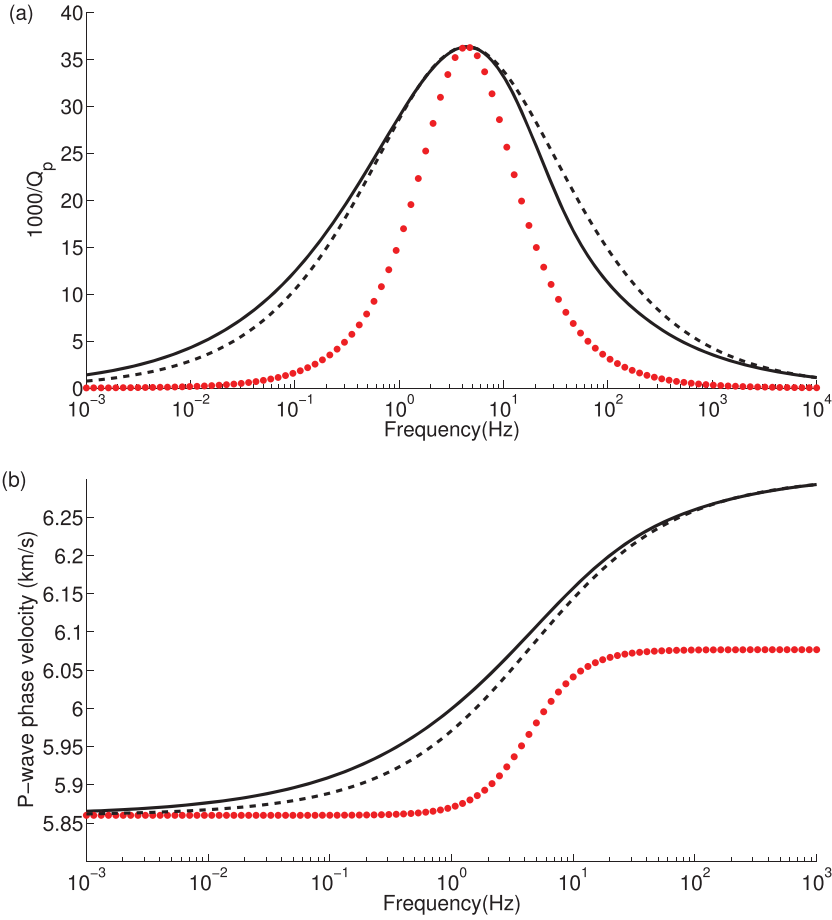


**Figure 4.** Dissipation factor (a) and phase velocity (b) of P-waves as a function of frequency for the random case (black-solid). The thickness is  $h=0.8$  mm. The Zener (red-dotted) and Cole–Cole (black-dashed) curves are shown.

### 2.3. Phase velocity

We obtain the phase velocity and stiffness modulus by using an approximation reported by Ref. [24] based on the Kramers–Kronig relations [20]. The phase velocity is given by

$$\frac{v_p(\omega)}{v_0} = \left( 1 - \frac{1}{\pi} \int_{\omega_0}^{\omega} \frac{Q^{-1}(\omega')}{\omega'} d\omega' \right)^{-1}, \quad (5)$$

where  $v_0$  is the reference velocity at  $\omega_0$ , which can be assumed as a very low-frequency value ( $\omega_0 \approx 0$ ). The complex wave modulus can be obtained from the phase velocity and  $Q$  factor as

$$M(\omega) \approx \rho v_p^2(\omega) \left( 1 + \frac{i}{Q(\omega)} \right), \quad (6)$$

where  $i = \sqrt{-1}$ .

## 3. Examples

We consider the solution for the P-wave quality factor of a sequence of layers with a periodic and random distribution of the properties, corresponding to the solution reported by Ref.[4, Eqs. (26 and 54)] (see [Appendix A](#)). As shown in [Figure 1](#), different shades of gray represent different

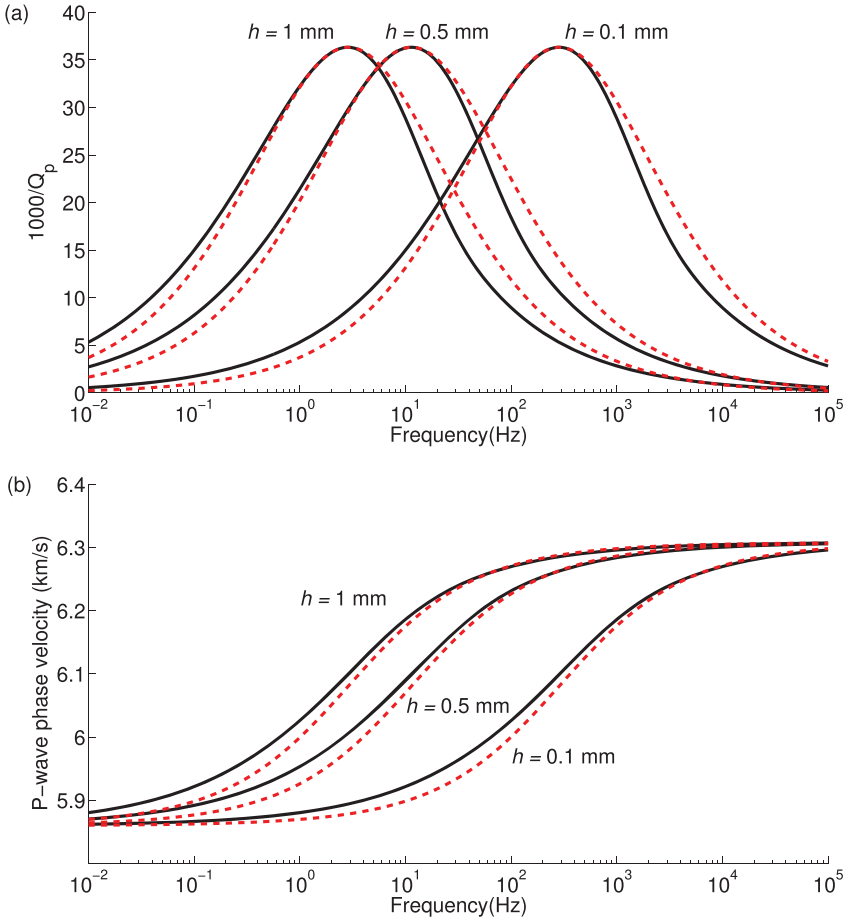


**Figure 5.** Dissipation factor (a) and phase velocity (b) of P-waves as a function of frequency for the random case and several layer thicknesses (black-solid curves). The dashed-red curves correspond to the Cole–Cole model.

media, where only the Grüneisen ratio ( $\Gamma$ ) varies. **Figure 1a** shows a periodic sequence of flat slabs of equal thickness  $h$  with properties labeled [1] and [2] (two media). **Figure 1b** illustrates a random model in which the thermoelastic properties of each slab are allowed to be different and their thickness is  $h$ .

**Figure 2** displays the dissipation factor and phase velocity of the P waves as a function of frequency for the periodic case. Increasing the thickness ( $h = 1, 2$  and  $5$  mm), the peak of attenuation moves to the low frequencies, without affecting the peak quality factor, and the velocity of the full frequency band increases gradually, while the low- and high-frequency limits velocity are the same.

The slabs of the random model can be arranged as shown in **Figures 1c** and **1d**, containing two and three different media, respectively. Basically, the proportion of media 1 and 2 in **Figure 1c** is the same as in **Figure 1a** (stationarity). For a uniform layer thickness,  $Q_R$  in Eq. (A.1) can be obtained exactly, giving  $Q_{p0}/2$ . Let us consider the model with two slabs of different properties. We assume the following properties:  $T_0 = 300$  K,  $K = 39$  GPa,  $\rho = 2650$  kg m $^{-3}$ ,  $c = 106 \times 10^6$  kg m $^{-2}$  s $^{-2}$  K $^{-1}$ ,  $\gamma = 532$  m kg s $^{-3}$  K $^{-1}$  and  $\mu = 39$  GPa. The two layers have  $\Gamma_1 = 1.1$  and  $\Gamma_2 = 2$ , and the thickness of each sheet is  $h = 0.8$  mm for the periodic and random cases. **Figure 3** compares the periodic and random cases (related to **Figures 1a** and **1c**) showing that in the second case, the peak is wider, shifted to low frequencies and asymmetric, the cases are similar to

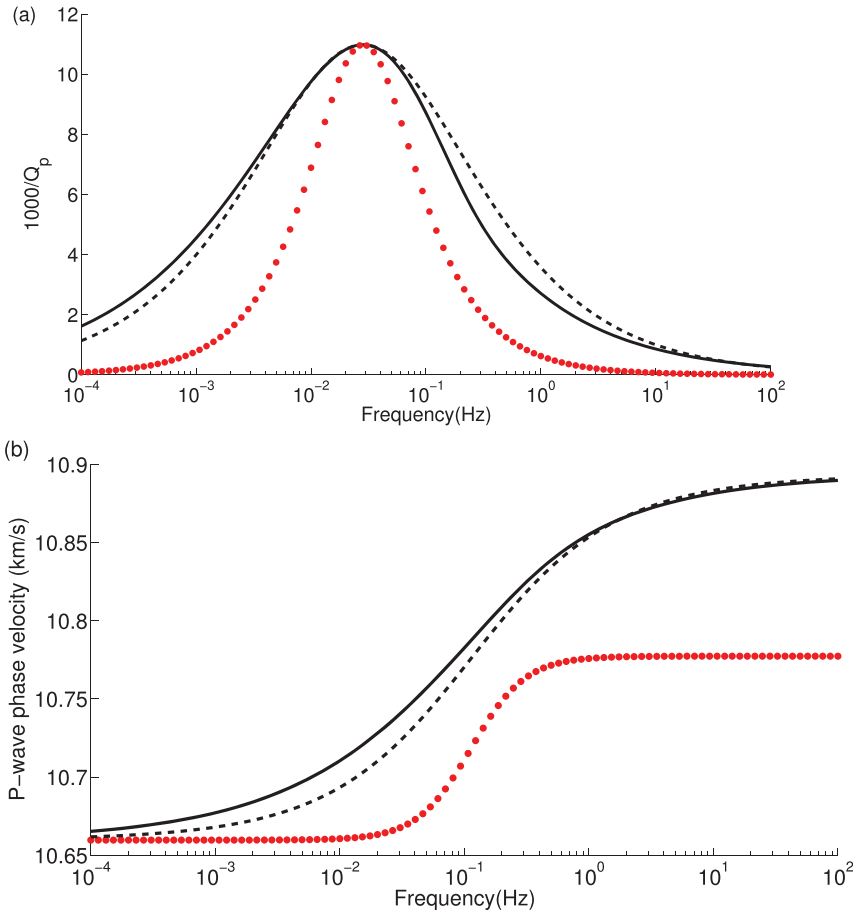


**Figure 6.** Dissipation factor (a) and phase velocity (b) of P-waves as a function of frequency for the random case (black solid). The thickness is  $h = 1$  mm. The Zener (red-dotted) and Cole–Cole (black-dashed) curves are shown. The thermoelastic properties correspond to the Earth’s mantle [30].

the experimental result in Ref. [29], that is, the trend and symmetry of curve. This is probably due to the further distribution in grain size, along with the neglected effect of elastic modulus relaxation [4]. The velocities coincide at the low-frequency limit.

Next, we consider the model shown in Figure 1d, the Grüneisen ratio  $\Gamma_1 = 1.1$ ,  $\Gamma_2 = 2$ ,  $\Gamma_3 = 1.5$ , and  $h = 0.8$  mm. Figure 4 compares the quality factors and phase velocities obtained with the random model to those of the Zener and Cole–Cole models, where we observe that the second provides a better approximation. We have used  $f_0 = 4.43$  Hz,  $Q_0 = 27.5$ , and  $r = 0.6$ . The Zener model matches the maximum value and location of the peak, but not its shape. The differences of Cole–Cole model from those of Zener model are explained using nonlinear internal friction within the rock [37], therefore, the Cole–Cole model gives a better fitting result and a better description of the physics of attenuation and dispersion [38].

Figure 5 illustrates the effect of the layer thickness and comparisons to the Cole–Cole model. Increasing the thickness ( $h = 0.1, 0.5$ , and  $1$  mm), the peak moves to the low frequencies, without affecting the peak quality factor, in agreement with results presented by Ref. [4, Eq. 54]. The Cole–Cole model parameters are:  $f_0 = 285$  Hz,  $11.4$  Hz and  $2.9$  Hz for  $h = 0.1, 0.5$ , and  $1$  mm, respectively,  $r = 0.58$  and  $Q_0 = 27.5$ . The velocities show the same low- and high-frequency limits irrespective of the thickness.

Finally, we consider a realistic set of properties with three layers, related to the Earth's mantle and based on Table 5 in Ref. [30] (MgSiO<sub>3</sub> perovskite). We assume  $T_0 = 500$  K,  $\alpha = 0.00218$  K<sup>-1</sup>,  $K = 257.9$  GPa,  $\rho = 4087$  kg m<sup>-3</sup>,  $c = 415.65 \times 10^6$  kg m<sup>-1</sup> s<sup>-2</sup> K<sup>-1</sup>,  $\gamma = 20.5$  m kg s<sup>-3</sup> K<sup>-1</sup> [31] and  $\mu = 3K/5$  (a Poisson medium). Moreover,  $\Gamma_1 = 1.37$ ,  $\Gamma_2 = 1.8$  and  $\Gamma_3 = 1.5$ , with  $h = 1$  mm. Figure 6 shows the results compared to those of the phenomenological Zener and Cole–Cole models. The peak quality factor is  $1000/10.98 \approx 91$  at a frequency of 0.11 Hz, which is consistent with the experimental values for the mantle [32, 33].

## 4. Conclusions

We have obtained analytical solutions of thermoelastic wave propagation in finely layered media with periodic and random variations of the thermal properties, specifically, the Grüneisen ratio. The solutions provide the quality factor and phase velocity as a function frequency, the latter computed with the Kramers–Kronig relations. The results are compared to those of the phenomenological Zener and Cole–Cole models, with the last one showing a very good fit. These approximations are required to compute wave fields in the space-time domain, using memory variables in the first case and fractional derivatives in the second case. For a succession of thin layers with a random distribution, the relaxation peak is wider and asymmetric compared to the ideal periodic case. In all the examples, the relaxation frequency of the random case is lower than that of the periodic case. An example based on realistic thermoelastic properties (Earth's mantle) gives a P-wave quality factor in agreement with experimental data.

## Appendix A thermoelastic attenuation

We consider a periodic system of alternating layers (slabs) each with thickness  $h$ , much smaller than the signal wavelength. We assume that the attenuation is small, that is,  $Q \gg 1$ . Ref. [4] obtained the relaxation peak caused by the passage of a P wave when a temperature gradient is induced. For clarity, we compare our notation with that of Armstrong. The equivalence is  $T \leftrightarrow T_0$ ,  $\rho c^2 \leftrightarrow E$ ,  $c_v \leftrightarrow c$ ,  $\gamma \leftrightarrow \Gamma$ ,  $\chi \leftrightarrow \gamma/c$ ,  $\Omega \leftrightarrow \omega$ ,  $s \leftrightarrow h$ ,  $s/\delta \leftrightarrow q$  and  $\kappa \leftrightarrow \gamma$ , where the left-hand side properties correspond to those of Armstrong. He presents the equations for the case where only the (dimensionless) Grüneisen ratio

$$\Gamma = \frac{\beta}{c} \quad (\text{A.1})$$

varies. Continuity of temperature and thermal current at the interfaces is required.

For periodic layering, the P-wave quality factor is

$$Q_P = \frac{q(\cosh q + \cos q)}{\sinh q - \sin q} \cdot Q_{P0}, \quad q = h\sqrt{\frac{\omega c}{2\gamma}}, \quad (\text{A.2})$$

where

$$Q_{P0} = \frac{4E}{cT_0(\Gamma_2 - \Gamma_1)^2}, \quad E = K + \frac{4}{3}\mu, \quad (\text{A.3})$$

where  $K = \lambda + 2\mu/3$  is the bulk modulus and  $E$  is the relaxed P-wave modulus.

For random variations of the Grüneisen ratio,  $\Gamma_j$ ,  $j = 1, \dots, L$  ( $L$  is the number of slabs where the average is applied), we have

$$Q_P = \frac{q}{3} \cdot [1 - \exp(-q)(\sin q + \cos q)]^{-1} \cdot Q_R, \quad (\text{A.4})$$

where

$$Q_R = \frac{2E}{cT_0 \langle (\Gamma - \bar{\Gamma})^2 \rangle}, \quad (\text{A.5})$$

where  $\bar{\Gamma}$  is the volume average obtained from the single  $\Gamma_j$  and the brackets take a volume average over all the layers.

## Appendix B Zener mechanical model

The Zener or standard-linear-solid model can be used to approximate the quality factors. The complex modulus of the Zener model is

$$M(f) = \frac{Q_0 + i(f/f_0)(R+1)}{Q_0 + i(f/f_0)(R-1)} \cdot M_0, R = \sqrt{1 + Q_0^2}, \quad (\text{B.1})$$

where  $f_0$  is the relaxation frequency,  $Q_0$  is the minimum quality factor at  $f_0$ ,  $M_0$  is the zero-frequency modulus,  $f$  is the frequency and  $i = \sqrt{-1}$ . The unrelaxed modulus ( $f \rightarrow \infty$ ) is  $M_\infty = [(R+1)/(R-1)]M_0$ , and the following relations hold,  $Q_0 = 2\sqrt{M_\infty M_0}/(M_\infty - M_0)$ , so that the modulus dispersion  $M_\infty - M_0$  can approximately be obtained from  $Q_0$ . Equation (B.1) was established by Ref. [34] for a rod of arbitrary cross-section vibrating transversely, where  $M_0$  and  $M_\infty$  correspond to the isothermal and adiabatic moduli, respectively [35, 36, Eq. 3.41].

The Zener  $Q$  factor is

$$Q(z) = \frac{\text{Re}(M)}{\text{Im}(M)} = \frac{Q_0}{2} \cdot \frac{1 + (f/f_0)^2}{f/f_0}, \quad (\text{B.2})$$

and the phase velocity is

$$v_p = \left[ \text{Re} \left( \frac{1}{v_c} \right) \right]^{-1}, v_c = \sqrt{\frac{M}{\rho}}, \quad (\text{B.3})$$

where  $v_c$  is the complex velocity [36].

## Appendix C Cole–Cole model

The Zener model can be generalized by using the Cole–Cole model [36], which involves derivatives of fractional order and is used to describe dispersion and energy loss in dielectrics, anelastic media and electric networks. The complex modulus of a Cole–Cole element is

$$M(\omega) = M_0 \cdot \frac{1 + (i\omega\tau_\epsilon)^r}{1 + (i\omega\tau_\sigma)^r}, \omega = 2\pi f, \quad (\text{C.1})$$

where  $0 < r < 2$  is a real number (the order of the derivative), the relaxation times are

$$\tau_\epsilon = \frac{a^{1/r}}{2\pi f_0}, \text{ and } \tau_\sigma = \frac{a^{-1/r}}{2\pi f_0}, \quad (\text{C.2})$$

where

$$a = \frac{1 + \sqrt{1 + Q_0^2} \sin \phi}{Q_0 \sin \phi - \cos \phi}, \phi = \frac{\pi r}{2}. \quad (\text{C.3})$$

The quality factor has a minimum value located at  $f_0 = [2\pi\sqrt{\tau_\epsilon\tau_\sigma}]^{-1}$ , as in the Zener case. The unrelaxed modulus is  $M_\infty = M_0(\tau_\epsilon/\tau_\sigma)^r$ . When  $r=1$ , we obtain the Zener model. This additional parameter is closely related to the width of the relaxation peak and allows us to fit better the thermoelastic relaxation peak.

## Funding

The authors are grateful for the support of National Natural Science Foundation of China (Grant No. 42104112), the Natural Science Foundation of Shandong Province (Grant No. ZR2021QD040), the China Postdoctoral Science Foundation (Grant No. 2021M703582), the Fundamental Research Funds for the Central Universities (Grant No. 20CX06087A), and 111 project “Deep-Superdeep Oil & Gas Geophysical Exploration” (B18055).

## References

- [1] C. Zener, “Internal friction in solids II. General theory of thermoelastic internal friction,” *Phys. Rev.*, vol. 53, no. 1, pp. 90–99, 1938. DOI: [10.1103/PhysRev.53.90](https://doi.org/10.1103/PhysRev.53.90).

- [2] S. Treitel, "On the attenuation of small-amplitude plane stress waves in a thermoelastic solid," *J. Geophys. Res.*, vol. 64, no. 6, pp. 661–665, 1959. DOI: [10.1029/JZ064i006p00661](https://doi.org/10.1029/JZ064i006p00661).
- [3] J. C. Savage, "Thermoelastic attenuation of elastic waves by cracks," *J. Geophys. Res.*, vol. 71, no. 16, pp. 3929–3938, 1966. DOI: [10.1029/JZ071i016p03929](https://doi.org/10.1029/JZ071i016p03929).
- [4] B. H. Armstrong, "Models for thermoelastic in heterogeneous solids attenuation of waves," *Geophysics*, vol. 49, no. 7, pp. 1032–1040, 1984. DOI: [10.1190/1.1441718](https://doi.org/10.1190/1.1441718).
- [5] M. A. Biot, "Thermoelasticity and irreversible thermodynamics," *J. Appl. Phys.*, vol. 27, no. 3, pp. 240–253, 1956. DOI: [10.1063/1.1722351](https://doi.org/10.1063/1.1722351).
- [6] H. W. Lord and Y. Shulman, "A generalized dynamical theory of thermoelasticity," *J. Mech. Phys. Solids*, vol. 15, no. 5, pp. 299–309, 1967. DOI: [10.1016/0022-5096\(67\)90024-5](https://doi.org/10.1016/0022-5096(67)90024-5).
- [7] A. E. Green and K. A. Lindsay, "Thermoelasticity," *J Elasticity*, vol. 2, no. 1, pp. 1–7, 1972. DOI: [10.1007/BF00045689](https://doi.org/10.1007/BF00045689).
- [8] A. E. Green and P. M. Naghdi, "Thermoelasticity without energy dissipation," *J Elasticity*, vol. 31, no. 3, pp. 189–208, 1993. DOI: [10.1007/BF00044969](https://doi.org/10.1007/BF00044969).
- [9] R. B. Hetnarski and J. Ignaczak, "On soliton-like thermoelastic waves," *Appl. Anal.*, vol. 65, no. 1-2, pp. 183–204, 1997. DOI: [10.1007/978-94-007-2739-7-921](https://doi.org/10.1007/978-94-007-2739-7-921).
- [10] D. S. Chandrasekharaiah, "Hyperbolic thermoelasticity: A review of recent literature," *Appl. Mech. Rev.*, vol. 51, no. 12, pp. 705–729, 1998. DOI: [10.1115/1.3098984](https://doi.org/10.1115/1.3098984).
- [11] D. Y. Tzou, "A unified field approach for heat conduction from macro-to micro-scales," *J. Heat. Transf.*, vol. 117, no. 1, pp. 8–16, 1995. DOI: [10.1115/1.2822329](https://doi.org/10.1115/1.2822329).
- [12] J. M. Carcione, Z. W. Wang, W. Ling, E. Salusti, J. Ba and L. Y. Fu, "Simulation of wave propagation in linear thermoelastic media," *Geophysics*, vol. 84, no. 1, pp. T1–T11, 2019a. DOI: [10.1190/geo2018-0448.1](https://doi.org/10.1190/geo2018-0448.1).
- [13] J. M. Carcione, F. Cavallini, E. Wang, J. Ba and L. Y. Fu, "Physics and simulation of wave propagation in linear thermoporoelastic media," *J. Geophys. Res. Solid Earth*, vol. 124, no. 8, pp. 8147–8166, 2019c. DOI: [10.1029/2019JB017851](https://doi.org/10.1029/2019JB017851).
- [14] Z. W. Wang, L. Y. Fu, J. Wei, W. T. Hou, J. Ba and J. M. Carcione, "On the Green function of the Lord-Shulman thermoelasticity equations," *Geophys. J. Int.*, vol. 220, no. 1, pp. 393–403, 2020. DOI: [10.1093/gji/ggz453](https://doi.org/10.1093/gji/ggz453).
- [15] J. Wei, L. Y. Fu, Z. W. Wang, J. Ba and J. M. Carcione, "Green function of the Lord-Shulman thermo-poroelasticity theory," *Geophys. J. Int.*, vol. 221, no. 3, pp. 1765–1776, 2020. DOI: [10.1093/gji/ggaa100](https://doi.org/10.1093/gji/ggaa100).
- [16] E. Wang, J. M. Carcione, F. Cavallini, M. A. B. Botelho and J. Ba, "Generalized thermo-poroelasticity equations and wave simulation," *Surv Geophys.*, vol. 42, no. 1, pp. 133–157, 2021. DOI: [10.1007/s10712-020-09619-z](https://doi.org/10.1007/s10712-020-09619-z).
- [17] G. Bonnet, "Basic singular solutions for a poroelastic medium in the dynamic range," *J. Acous. Soc. Am.*, vol. 82, no. 5, pp. 1758–1762, 1987. DOI: [10.1121/1.395169](https://doi.org/10.1121/1.395169).
- [18] A. Norris, "On the correspondence between poroelasticity and thermoelasticity," *J. Appl. Phys.*, vol. 71, no. 3, pp. 1138–1141, 1992. DOI: [10.1063/1.351278](https://doi.org/10.1063/1.351278).
- [19] Y. Gueguen, "Wave propagation and attenuation in rocks from poroelasticity and thermoelasticity," *Poromechanics V: Proceedings of the Fifth Biot Conference on Poromechanics*, 2013. DOI: [10.1061/9780784412992.279](https://doi.org/10.1061/9780784412992.279).
- [20] J. M. Carcione, D. Gei, J. E. Santos, L. Y. Fu and J. Ba, "Canonical analytical solutions of wave-induced thermoelastic attenuation," *Geophys. J. Int.*, vol. 221, no. 2, pp. 835–842, 2020a. DOI: [10.1093/gji/ggaa033](https://doi.org/10.1093/gji/ggaa033).
- [21] C. Zener, *Elasticity and Anelasticity of Metals*. Chicago: The University of Chicago press., 1948.
- [22] J. M. Carcione, F. Mainardi, S. Picotti, L. Y. Fu and J. Ba, "Thermoelasticity models and P-wave simulation based on the Cole–Cole model," *J. Therm. Stresses*, vol. 43, no. 4, pp. 512–527, 2020b. DOI: [10.1080/01495739.2020.1722772](https://doi.org/10.1080/01495739.2020.1722772).
- [23] J. M. Carcione, S. Picotti and J. Ba, "P- and S-wave simulation using a Cole–Cole model to incorporate thermoelastic attenuation and dispersion," *J Acoust Soc Am*, vol. 149, no. 3, pp. 1946–1954, 2021. DOI: [10.1121/10.0003749](https://doi.org/10.1121/10.0003749).
- [24] M. O'Donnell, E. T. Jaynes and J. G. Miller, "Kramers–Kronig relationship between ultrasonic attenuation and phase velocity," *J. Acoust. Soc. Am.*, vol. 69, no. 3, pp. 696–701, 1981. DOI: [10.1121/1.385566](https://doi.org/10.1121/1.385566).
- [25] J. M. Carcione, F. Cavallini, J. Ba, W. Cheng and A. N. Qadrouh, "On the Kramers–Kronig relations," *Rheol Acta*, vol. 58, no. 1-2, pp. 21–28, 2019b. DOI: [10.1007/s00397-018-1119-3](https://doi.org/10.1007/s00397-018-1119-3).
- [26] L. Anderson, "Bulk attenuation in the Earth and viscosity of the core," *Nature*, vol. 285, no. 5762, pp. 204–207, 1980. DOI: [10.1038/285204a0](https://doi.org/10.1038/285204a0).
- [27] B. Budiansky, E. E. Sumner, Jr and R. J. O'Connell, "Bulk thermoelastic attenuation of composite materials," *J. Geophys. Res.*, vol. 88, no. B12, pp. 10343–10348, 1983. DOI: [10.1029/JB088iB12p10343](https://doi.org/10.1029/JB088iB12p10343).
- [28] J. X. Wei and B. R. Di, "The experimental studies on influence of periodic layered media to P-wave velocity," *Oil Geophysical Prospecting*, vol. 45, no. 5, pp. 661–666, 2010. DOI: [10.1017/S0004972710001772](https://doi.org/10.1017/S0004972710001772).

- [29] R. H. Randall, F. C. Rose and C. Zener, "Intercrystalline thermal currents as a source of internal friction," *Phys. Rev.*, vol. 56, no. 4, pp. 343–348, 1939. DOI: [10.1103/PhysRev.56.343](https://doi.org/10.1103/PhysRev.56.343).
- [30] O. L. Anderson, "The Grüneisen ratio for the last 30 years," *Geophys. J. Int.*, vol. 143, no. 2, pp. 279–294, 2000. DOI: [10.1046/j.1365-246X.2000.01266.x](https://doi.org/10.1046/j.1365-246X.2000.01266.x).
- [31] V. Haigis, M. Salanne and S. Jahn, "Thermal conductivity of MgO, MgSiO<sub>3</sub> perovskite and post-perovskite in the Earth's deep mantle," *Earth. Planet. Sc. Lett.*, vol. 355-356, pp. 102–108, 2012. DOI: [10.1016/j.epsl.2012.09.002](https://doi.org/10.1016/j.epsl.2012.09.002).
- [32] F. Birch, J. F. Schairer and H. C. Spicer, *Handbook of Physical Constants*. Baltimore: Geological Society of America, 1942.
- [33] B. Romanowicz and B. Mitchell, "Deep Earth structure: Q of the Earth from crust to core," *Treatise Geophysics*, vol. 1, no. 25, pp. 789–827, 2015. DOI: [10.1016/B978-0-444-53802-4.00021-X](https://doi.org/10.1016/B978-0-444-53802-4.00021-X).
- [34] C. Zener, "Internal friction in solids. I. Theory of internal friction in reeds," *Phys. Rev.*, vol. 52, no. 3, pp. 230–235, 1937. DOI: [10.1103/PhysRev.52.230](https://doi.org/10.1103/PhysRev.52.230).
- [35] F. Mainardi, "Fractional calculus and waves in linear viscoelasticity: An introduction to mathematical models," *World Scientific*, 2010. DOI: [10.1007/978-3-7091-2664-6-7](https://doi.org/10.1007/978-3-7091-2664-6-7).
- [36] J. M. Carcione, *Wave Fields in Real Media. Theory and Numerical Simulation of Wave Propagation in Anisotropic, Anelastic, Porous and Electromagnetic Media*, 3rd ed. New York: Elsevier. (extended and revised), 2014.
- [37] W. B. Deng and I. B. Morozov, "Mechanical interpretation and generalization of the Cole–Cole model in viscoelasticity," *Geophysics*, vol. 83, no. 6, pp. MR345–MR352, 2018. DOI: [10.1190/geo2017-0821.1](https://doi.org/10.1190/geo2017-0821.1).
- [38] S. Picotti and J. M. Carcione, "Numerical simulation of wave-induced fluid flow seismic attenuation based on the Cole–Cole model," *J. Acous. Soc. Am.*, vol. 142, no. 1, pp. 134–145, 2017. DOI: [10.1121/1.4990965](https://doi.org/10.1121/1.4990965).